Available online at www.sciencedirect.com
ScienceDirect
Ceramics International 36 (2010) 2359–2364
CERAMICS INTERNATIONAL
www.elsevier.com/locate/ceramint

Growth-temperature-dependent microstructure and ferromagnetic properties of perovskite manganite-based heterostructures

Yuan-Chang Liang *

Institute of Materials Engineering, National Taiwan Ocean University, No. 2, Peining Road, Keelung City 20224, Taiwan

Received 24 February 2010; received in revised form 11 May 2010; accepted 10 June 2010
Available online 3 August 2010

Abstract

Oxide heterostructures composed of ferromagnetic $La_{0.7}Ba_{0.3}MnO_3$ (LBMO) spacers and paramagnetic $LaNiO_3$ (LNO) spacers were grown on $SrTiO_3$ (0 0 1) substrates at various substrate temperatures. The X-ray diffraction (XRD) patterns confirm the formation of the heterostructure at a growth temperatures of 400–600 °C. A high substrate temperature of 700 °C caused serious atomic intermixing between the LBMO and the LNO spacers of the heterostructure, further degrading the crystalline quality of the heterostructure. The ferromagnetic LBMO spacer in the heterostructure is under biaxial compressive stress. The XRD results reveal that the lattice of the heterostructure was elongated parallel to the *c*-axis at a growth temperature of 400–600 °C. Experiments that involve XRD, atomic force microscopy and X-ray photoelectron spectroscopy provide structural information on the designed heterostructures. The observed magnetization characteristics of the heterostructures show that lattice strain and the quality of the surface and the interface of heterostructures affect the Curie temperature of the manganite layers.

Keywords: A. Films; B. Surfaces; D. Perovskites

1. Introduction

The colossal magnetoresistance (CMR) in half-metal oxide manganite compounds has been extensively investigated [1–4]. Because of their electrical, transport, and magnetic properties, manganites are a very interesting class of model materials for studying magnetism and also because of their possible use in innovative magnetic devices. Doped perovskite manganites $R_{1-x}A_xMnO_3$, in which some of the trivalent rare-earth ions R^{3+} are replaced by divalent alkaline-earth metal ions A^{2+}, have been examined extensively in recent years, since they exhibit an interesting metal–insulator transition [5,6]. In several experiments on ultra-thin single films or manganite-insulator multilayers, a loss in magnetic moment, a drop in the metal to insulator transition temperature and the Curie temperature, and an increase in resistivity are observed [7,8]. Strain caused by a lattice mismatch and lattice distortions that are caused by the thickness of film are well known to affect strongly the properties of manganite thin films [9]. Processes parameters also reportedly influence the magnetic and transport properties of the manganites even when their doping level is fixed [10–12]. Recently, some novel properties were observed in CMR thin films [13], indicating that the strain effect can be utilized to tailor or optimize the magnetic and transport properties of CMR thin films, even though this effect is still not thoroughly understood. Recently, (La,Ba)MnO_3(LBMO) manganite has received much attention because of its anomalous magnetic properties [14]. A detailed study of strained LBMO thin film may promote an understanding of the strain effect and, further the potential application in devices. This work investigates systematically the magnetic properties of various strained LBMO thin films with LBMO/$LaNiO_3$(LNO) asymmetric heterostructures. The LNO was used because it has satisfactory crystallographic compatibility for heteroepitaxial growth of a perovskite layer [15]; moreover, LNO is a paramagnetic oxide. The effect of growth temperature on the strain state in the heterostructure was systemically investigated. The correlation between the strain size and the magnetization characteristics of the LBMO/LNO heterostructure was reported.

2. Experiments

In order to investigate the growth temperature effect on the microstructure and physical properties of the manganites, the

* Tel.: +886 2 24622192; fax: +886 2 24620724.
E-mail address: yuanvictory@gmail.com.

0272-8842/$36.00
doi:10.1016/j.ceramint.2010.07.025

heterostructures with $(LBMO_m/LNO_n)_{12}$ in which $m = 8$ and $n = 2$ nm are adopted in this work. Single crystal $SrTiO_3$ (STO) with (1 0 0)-orientation was used as a substrate. During deposition, the substrate temperature was kept at various temperatures (400–700 °C). The gas pressure of deposition was fixed at 10 mTorr with an Ar/O_2 ratio of 4:1. The deposition plasma powers are fixed at ~2.96 W/cm^2 for the LBMO and the LNO films.

The crystallographic structures and strain states of the heterostructures were analyzed by measurements of high resolution X-ray diffraction (XRD). The surface morphology of the heterostructure was investigated with an atomic force microscopy (AFM). The chemical composition of the as-deposited manganite films was determined using X-ray photoelectron spectroscopy (XPS). A superconducting quantum-interference device magnetometer was used to measure the magnetization of the samples.

3. Results and discussion

Fig. 1(a) exhibits (0 0 L) crystal truncation rod (CTR) intensity profiles of the heterostructures grown at 400–600 °C. For simplicity, the value of L given in this paper is expressed in reciprocal lattice units (r.l.u.) referred to the STO lattice parameter (0.3905 nm near 295 K). The (0 0 2) XRD spectra of the heterostructures show a well-defined (0 0 2) zeroth-order peak with well-resolved satellites on both sides, revealing their highly crystalline quality. In particular, the observed satellites in the XRD patterns reveal the high quality of the heterointerface of the heterostructure. However, the heterostructure that was grown at 700 °C was not strongly layered, according to the results of XRD. No differentiable main peak or satellite peak was observed in the XRD pattern, indicating that a high growth temperature of 700 °C reduced the crystalline quality of the heterostructure in this work. This might be due to the serious atomic intermixing between the LBMO and the LNO spacers at the high growth temperature. Moreover, the high growth temperature is posited to result in a loss of Ni in the deposited LNO film; this might further deteriorate the crystalline quality of the heterostructure [16]. In the heterostructure, the LBMO spacer is in a biaxial compressive state, whereas the LNO sublayer is in a biaxial tensile state (theoretical bulk lattice parameters: $a_{LBMO} = 0.392$ nm and $a_{LNO} = 0.3887$ nm). The position of the zeroth-order peak in CTR spectra can be determined by the average c-axis length of the heterostructure from the Vegard's law [17]. The average c-axis length of the heterostructure can be determined by the equation of $c = L\lambda/2 \sin\theta$, where L is the location of the Bragg reflection expressed in reciprocal lattice unit (r.l.u.) and θ the measured Bragg angle, here the spacing of the (0 0 2) planes is probed. The determined average c-axis lattice length of the heterostructure increased from 0.392 to 0.394 nm with growth temperature from 400 °C to 600 °C, respectively. The mean lattice parameter c of the heterostructures is larger than the weighted mean of the lattice parameter c (0.391 nm) of unstrained LBMO and LNO films, suggesting an elongation of the average c-axis lattice of the heterostructure along [0 0 L] through heteroepitaxial strain in the heterostructure. The average c-axis lattice constant of the heterostructure grown at 700 °C is not determined because of the loss of a well-layered structure herein. The expression $(c - c_w)/c_w$ was used to determine the degree of elongation along the c-axis in the heterostructure owing to the strain effect. The term c represents the average length of the c-axis lattice in the heterostructure and is determined from the XRD patterns; c_w is the weighted mean of the lattice parameter c of unstrained LBMO and LNO films. From Fig. 2, a higher growth temperature is associated with a greater degree of straining

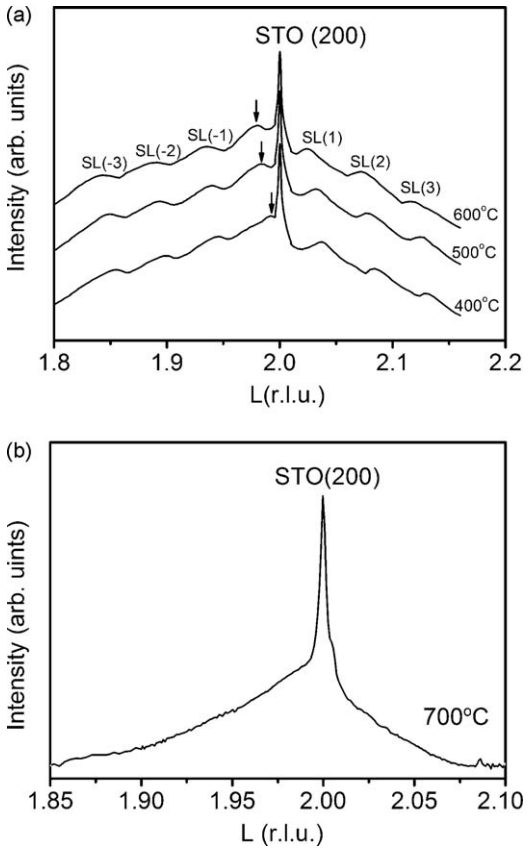

Fig. 1. (0 0 L) CTR intensity profiles of the heterostructures. (a) Heterostructures with a well-layered structure grown at 400–600 °C. The arrows represent the position of zeroth-order peak of the heterostructures. (b) Heterostructure without a well-layered structure grown at 700 °C.

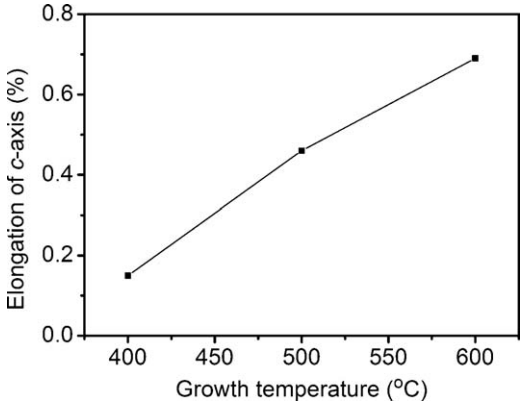

Fig. 2. The degree of elongation of c-axis lattice length of the heterostructures.

in the heterostructure, perhaps because the grains in the heterostructure were larger when the film was grown at a higher temperature; large grains are associated with better straining of the manganite in the heterostructure, because of mismatched lattices [18]. The results of XRD clearly show that these heterostructures exhibited various degrees of lattice distortion. The heterostructure grown at 600 °C exhibits the largest elongation along the *c*-axis lattice of any of the samples. Accordingly, the heterostructure that was grown at 600 °C had the longest Mn–O bond along *c*-axis lattice in the manganite spacers while that grown at 400 °C had the narrowest distribution of Mn–O bond lengths along *c*-axis lattice. Strain in the thin film structure may contribute significantly to the distortion of MnO_6 orchestra in the manganese films and further affect the physical properties of the manganites [19].

The epitaxy between the LBMO and the LNO spacers in the heterostructure is demonstrated by the in-plane orientation with respect to the major axes {1 0 2} of the STO substrate. The azimuthal (1 0 2) diffraction patterns of the heterostructure grown at 400 °C and 600 °C are shown in Fig. 3. No other peaks are observed in the intervals between the four peaks, indicating the well epitaxial nature between the LBNO and the LNO spacers grown on a STO substrate. The results of the XRD Phi-scans demonstrate that the use of an LNO buffer ensures that the heterostructure remains epitaxy over a wide range of growth temperatures.

Fig. 4(a) shows the survey scan of XPS spectra of the LBMO grown at 600 °C. XPS signals from La, Ba, Mn, and O were observed in the figure. The composition of the LBMO grown at various temperatures was determined from the narrow scans of XPS spectra. The compositions of the LBMO are determined to be La:Ba:Mn:O = 0.68:0.32:1.00:2.98 and are independent of growth temperature. The oxygen content in the manganite is close to the stoichiometric value. Fig. 4(b)–(d) presents the O1s core-level spectra of the LBMO that were grown at various temperatures. An almost symmetric peak was obtained from Fig. 4(b)–(d) at the same binding energy as an LBMO single crystal, suggesting that the LBMO had an almost microscopically homogeneous film structure. The peak at the higher binding energy is resulted from crystal defects in the LBMO and the intensity of the peak is quite small. Notably, the oxygen

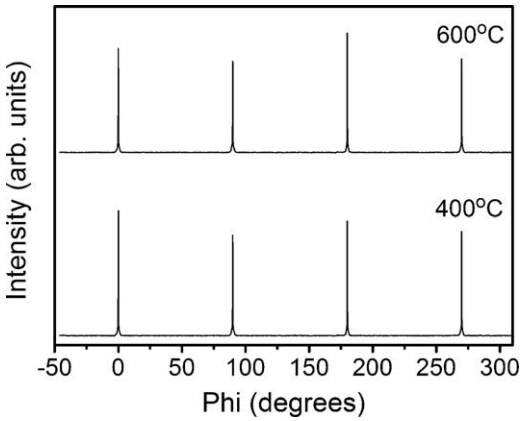

Fig. 3. Phi-scans of the (1 0 2) zeroth-order peak of the heterostructures grown at 400 °C and 600 °C.

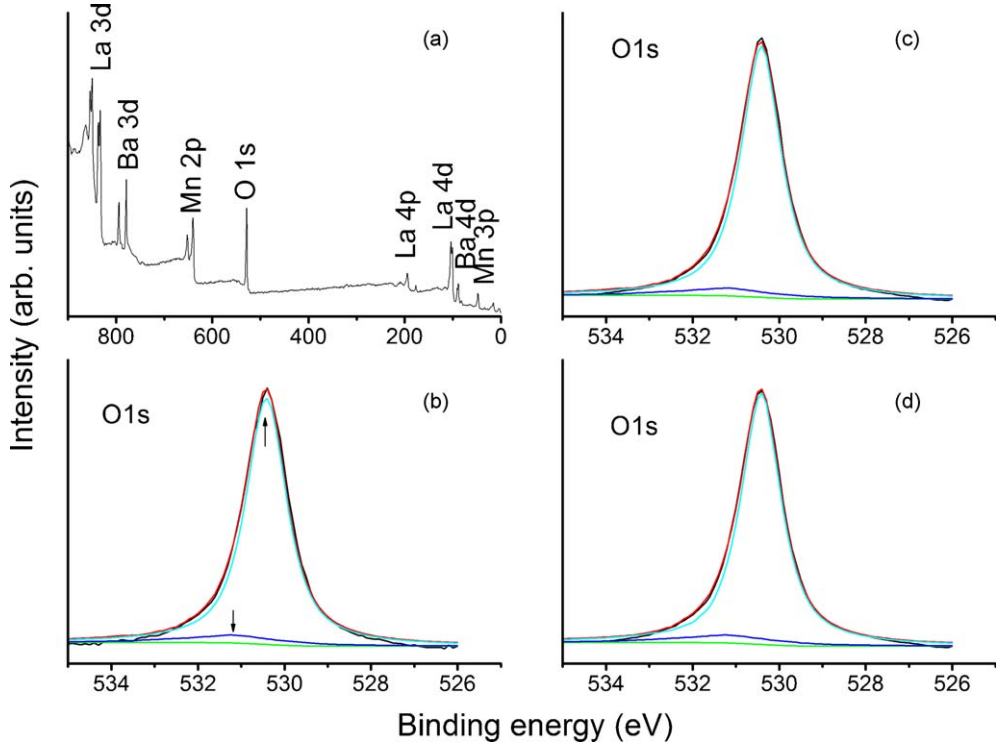

Fig. 4. (a) XPS survey spectrum of the LBMO grown at 600 °C. O1s core-level spectra of the LBMO layer in the heterostructure grown at various temperatures were shown in (b) 400 °C, (c) 500 °C and (d) 600 °C. The arrow at the higher binding energy indicates that the content of oxygen vacancy in the film is quite small and the arrow at the lower binding energy represents the crystal oxygen of the LBMO.

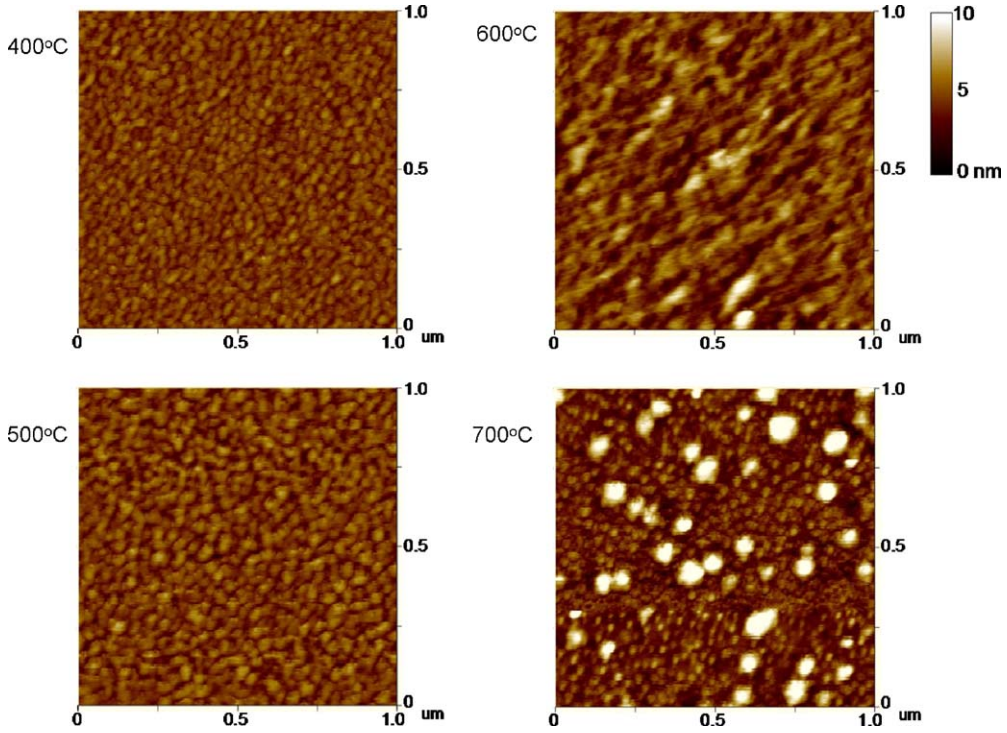

Fig. 5. Surface morphologies of the heterostructures grown at various temperatures.

content of the LBMO was independent of growth temperature, suggesting that the variation in the elongation of the average *c*-axis lattice length of the heterostructures that were grown at various temperatures results from lattice strain and not lattice defects.

Fig. 5 shows the surface morphology of the heterostructures grown at various temperatures. The heterostructures grown at 400–600 °C contain tiny three-dimensional (3D) grains on the surface. An apparent coarsening of the surface of the heterostructure that was grown at 700 °C was observed. The surface of the heterostructure appeared rather rough when it was grown at 700 °C; it contains large 3D grains, perhaps because of a serious atomic intermixing between the constituent spacers. Additionally, the initially rough surface of the LNO spacers that was grown at the high growth temperature may explain most of the roughening of the subsequently formed manganite films [20]. The heterostructures that were grown at 400–600 °C have relatively dense and smooth film surfaces. However, the root-mean-square (rms) surface roughness of the heterostructures grown at 700 °C was 1.93 nm. Large 3D islands were formed on the surface of the film, contributing to the roughness of its surface (Fig. 6).

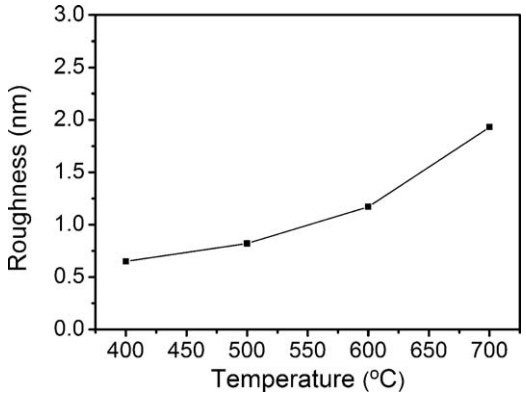

Fig. 6. Root-mean-square surface roughness of the heterostructures grown at various temperatures.

Fig. 7(a) displays the temperature dependence of magnetization of the heterostructures grown at various temperatures. All the magnetization vs. temperature curves show that the heterostructures are ferromagnetic coupling below the Curie temperature. The Curie temperature of the heterostructures was determined from the magnetization curves. Fig. 7(b) reveals that the Curie temperature of the heterostructures decreased from 252 to 201 K (by ∼20%) as the growth temperature increased from 400 °C to 600 °C. Orgiani et al. showed that, independently of whether the strain is compressive or tensile, the oxygen content dominates the magnetic properties of manganite films [21]. In this work, the oxygen contents of the manganite layers in the heterostructures grown at various temperatures are almost equal, and the oxygen content of the manganite is close to the stoichiometric value. Two factors may dominate the magnetic properties of the manganite heterostructures herein. First, the *c*-axis lattice elongation of the heterostructure increased from 0.15% to 0.69% as the growth temperature increased from 400 °C to 600 °C. Notably, the LNO spacer is a paramagnetic material. The magnetization of the heterostructure is caused by the LBMO spacers. The in-plane compressive strain of the LBMO spacer in the heterostructure that is caused by the insertion of the LNO spacer causes a measurable static anisotropic distortion of the

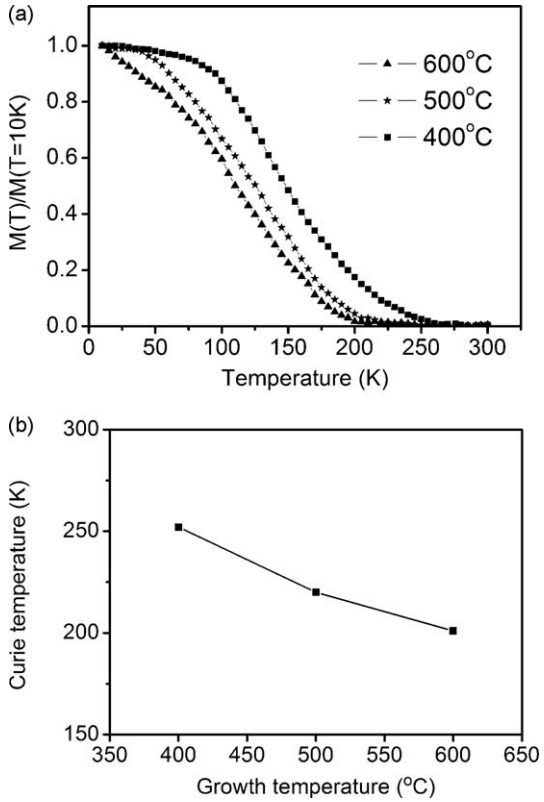

Fig. 7. (a) Temperature dependence of the normalized magnetization of the heterostructures. The data were obtained in a field of 1 T. (b) Curie temperature vs. growth temperature of the heterostructures.

MnO_6 octahedra in the LBMO spacers, with splitting of the in-plane and out-of-plane Mn–O bond lengths. This distortion may increase the splitting of the e_g levels, tending to localize the charge carriers [22]. The lattice strain may contribute to the suppression of ferromagnetism among these heterostructures. The heterostructure with a greater expansion of *c*-axis lattice exhibited a lower Curie temperature implying, macroscopically, that lattice strain in the heterostructure may significantly affect the Curie temperature. The similar strain effect on Curie temperature of manganite thin films has also been proposed by Chou et al. [23]. A suppressed charge carrier transfer resulting from strain-induced modification of Mn–O–Mn networks has also been posited to affect the magnetic properties of manganites [22,24]. Second, increasing the growth temperature might increase surface roughness of the film, as is revealed by the AFM images. The alternating stack of LBMOs and LNOs to form the heterostructure at a relatively high growth temperature may produce a rough interface in the heterostructure. The rough heterointerface may cause spin canting in the heterostructure further suppressing ferromagnetism [8]. The correlation between the magnetization and microstructures shows that lattice strain and structural quality of the LBMO surface and heterointerfaces reduce the Curie temperature of the manganites. The correlation between the microstructure and the physical properties of the manganite herein is important to tailoring the physical properties of manganite and using it in practical applications.

4. Conclusions

Variously strained heterostructures with alternating stacks of ferromagnetic LBMO and paramagnetic LNO spacers were successfully grown on STO substrates at various temperatures. The XRD results show that a high growth temperature of 700 °C degrades the crystalline quality of the heterostructures. The heterostructures that were grown at 400–600 °C have a well-layered structure with an epitaxial orientation between that of the LBMO and that of the LNO on STO substrates. The XRD results reveal a clear enhancement of the tetragonality of the LBMO lattice in the heterostructure owing to the misfit strain at the heterointerfaces. Higher growth temperature results in a larger elongation of the *c*-axis lattice of the heterostructures. The relationship between the microstructure and the Curie temperature of the heterostructures reveals that both the in-plane compressive strain and the quality of the surface and interface of the LBMO in the heterostructure affect the Curie temperature of the manganite. The results herein constitute a good reference for the design of novel devices based on manganite thin films.

Acknowledgements

The author would like to acknowledge the financial support from the National Science Council of the Republic of China (Grant No. NSC 97-2221-E-270-004) and the National Taiwan Ocean University (Grant No. NTOU-RD-AA-2010-104031).

References

[1] A. Barman, M. Ghosh, S. Biswas, S.K. De, S. Chatterjee, Electrical properties of $La_{0.6}Re_{0.1}Ca_{0.3}MnO_3$ (Re = Pr, Sm, Gd, Dy) at low temperature, Solid State Commun. 106 (1998) 691–694.

[2] A. Barman, M. Ghosh, S. Biswas, S.K. De, S. Chatterjee, Electrical and magnetic properties of $La_{0.7-x}Y_xSr_{0.3}MnO_3$ ($0 \leqq x \leqq 0.2$) perovskite at low temperature, J. Phys. Condens. Matter. 10 (1998) 9799–9812.

[3] P. Chen, D.Y. Xing, Y.W. Du, Positive magnetoresistance from quantum interference effects in perovskite-type manganites, Phys. Rev. B 64 (2001) 104402–104406.

[4] D. Kumar, J. Sankar, J. Narayan, R.K. Singh, A.K. Majumdar, Low-temperature resistivity minima in colossal magnetoresistive $La_{0.7}Ca_{0.3}MnO_3$ thin films, Phys. Rev. B 65 (2002) 094407–094412.

[5] M. Angeloni, G. Balestrino, N. Boggio, P.G. Medaglia, P. Orgiani, A. Tebano, Suppression of the metal–insulator transition temperature in thin $La_{0.7}Sr_{0.3}MnO_3$ films, J. Appl. Phys. 96 (2004) 6387–6392.

[6] A.Yu. Petrov, C. Aruta, S. Mercone, C. Adamo, I. Alessandri, L. Maritato, Room temperature metal–insulator transition in as grown $(La_{1-x}\ Sr_x)_y MnO_3$ thin films deposited by molecular beam epitaxy, Eur. Phys. J. B 40 (2004) 11–18.

[7] M. Izumi, Y. Ogimoto, Y. Okimoto, T. Manako, P. Ahmet, K. Nakajima, T. Chikyow, M. Kawasaki, Y. Tokura, Insulator–metal transition induced by interlayer coupling in $La_{0.6}Sr_{0.4}MnO_3/SrTiO_3$ superlattices, Phys. Rev. B 64 (2001) 064429–064434.

[8] R.A. Rao, D. Lavric, T.K. Nath, C.B. Eom, L. Wu, F. Tsui, Three-dimensional strain states and crystallographic domain structures of epitaxial colossal magnetoresistive $La_{0.8}Ca_{0.2}MnO_3$ thin films, Appl. Phys. Lett. 73 (1998) 3294–3296.

[9] F. Tsui, M.C. Smoak, T.K. Nath, C.B. Eom, Strain-dependent magnetic phase diagram of epitaxial $La_{0.67}Sr_{0.33}MnO_3$ thin films, Appl. Phys. Lett. 76 (2000) 2421–2423.

[10] J.Q. Guo, H. Takeda, N.S. Kazama, K. Fukamichi, M. Tachiki, Deposition conditions of magnetoresistance in $La_{0.67}Ca_{0.33}MnO_{3-\delta}$ thin film, J. Appl. Phys. 81 (1997) 7445–7449.

[11] W. Wu, K.H. Wong, C.L. Mak, G. Pang, C.L. Choy, Y. Zhang, Influence of oxygen background pressure on the structure and properties of epitaxial $SrTiO_3/La_{0.35}Nd_{0.35}Sr_{0.3}MnO_3$ heterostructures grown by pulsed laser deposition, J. Vac. Sci. Technol. A 18 (2000) 2378–2383.

[12] W. Wu, K.H. Wong, X.G. Li, C.L. Choy, Y. Zhang, Effect of annealing in reduced oxygen pressure on the electrical transport properties of epitaxial thin film and bulk $(La_{1-x}Nd_x)_{0.7}Sr_{0.3}MnO_3$, J. Appl. Phys. 87 (2000) 3006–3010.

[13] F.S. Razavi, G. Gross, H.-U. Habermeier, O. Lebedev, S. Amelinckx, G. Van Tendeloo, A. Vigliante, Epitaxial strain induced metal insulator transition in $La_{0.9}Sr_{0.1}MnO_3$ and $La_{0.88}Sr_{0.1}MnO_3$ thin films, Appl. Phys. Lett. 76 (2000) 155–157.

[14] H.L. Ju, Y.S. Nam, J.E. Lee, H.S. Shin, Anomalous magnetic properties and magnetic phase diagram of $La_{1-x}Ba_xMnO_3$, J. Magn. Magn. Mater. 219 (2000) 1–8.

[15] Y.C. Liang, H.Y. Lee, H.J. Liu, K.F. Wu, T.B. Wu, C.H. Lee, Evaluation of strain-dependent dielectric properties in $BaTiO_3/LaNiO_3$ and (Ba,Sr)-$TiO_3/LaNiO_3$ artificial superlattice films on $LaNiO_3$-coated $SrTiO_3$ substrates, J. Electrochem. Soc. 152 (2005) F129–F132.

[16] Y.C. Liang, Y.C. Liang, Effects of substrate temperature on the physical properties of strained $BaTiO_3/LaNiO_3$ artificial superlattices, J. Cryst. Growth 285 (2005) 345–351.

[17] B.D. Cullity, Elements of X-ray Diffraction, Addison-Wesley Publishing Company, Inc., 1978.

[18] Y.C. Liang, Y.C. Liang, J.P. Chu, Physical properties of strained $Ba_{0.5}Sr_{0.5}(Ti,Mn)O_3$ thin films buffered with $La_{0.68}Ba_{0.32}MnO_3$ conductive layers, Electrochem. Solid State Lett. 11 (2008) G41–G45.

[19] T.Y. Koo, S.H. Park, K.B. Lee, Y.H. Jeong, Anisotropic strains and magnetoresistance of $La_{0.7}Ca_{0.3}MnO_3$, Appl. Phys. Lett. 71 (1997) 977–979.

[20] N. Sugii, K. Takagi, Change in surface morphologies with pulsed-laser-deposition-temperature for $SrTiO_3$ and $Ba_{0.7}Sr_{0.3}TiO_3$ thin films on Pt electrodes, Thin Solid Films 323 (1998) 63–67.

[21] P. Orgiani, A. Guarino, C. Aruta, C. Adamo, A. Galdi, A.Yu. Petrov, R. Savo, L. Maritato, Magnetotransport properties of epitaxial strain-less $La_{0.7}Ba_{0.3}MnO_3$ thin films, J. Appl. Phys. 101 (2007) 033904.

[22] Y.C. Liang, Y.C. Liang, Quantifying strain effects on physical properties of $La_{0.68}Ba_{0.32}MnO_3$ epilayers and heterostructures, J. Electrochem. Soc. 154 (2007) P147–P151.

[23] H. Chou, M.H. Tsai, F.P. Yuan, S.K. Hsu, C.B. Wu, J.Y. Lin, C.I. Tsai, Y.H. Tang, Effects of strain on the electronic structures and T_C's of the $La_{0.67}Ca_{0.33}MnO_3$ and $La_{0.8}Ba_{0.2}MnO_3$ thin films deposited on $SrTiO_3$, Appl. Phys. Lett. 89 (2006) 082511.

[24] T. Kanki, T. Yanagida, B. Vilquin, H. Tanaka, T. Kawai, Hall effect in strained $La_{0.85}Ba_{0.15}MnO_3$ thin films, Phys. Rev. B 71 (2005) 012403.